

Daily peak-shaving model of cascade hydropower serving multi-grids considering an HVDC channel shared constraint

Shengli Liao^a, Hualong Yang^a, Benxi Liu^{a,*}, Hongye Zhao^a, Huan Liu^a, Xiangyu Ma^a, Huijun Wu^b

^a Institute of Hydropower and Hydroinformatics, Dalian University of Technology, Dalian, 116024, China

^b Power Dispatching Control Center of China Southern Power Grid, Guangzhou, 510623, China

ARTICLE INFO

Keywords:

Hydropower transmission
Multiple grids peak-shaving
Sharing HVDC channel
Constraint restructuring

ABSTRACT

High-voltage direct current (HVDC) is widely applied in large-scale hydropower transmission in China because of its long distance, large capacity and low power loss. However, when multiple hydropower stations send power by sharing one HVDC transmission channel, it is challenging to ensure the security of the sending-end power grid. To address this problem, a short-term peak-shaving model serving multiple power grids considering an HVDC channel shared (HCS) constraint is proposed. First, a daily peak-shaving model for cascade hydropower stations serving multiple power grids coupling with conventional HVDC constraints is established. Second, for the power transmission of different hydropower stations sharing one HVDC channel, the HCS constraint restructured by set-calculation is integrated into the model. Finally, the Big-M method is adopted to linearize the restructured HCS constraint to build an MILP model due to its flexibility in handling massive inequality constraints. The result from the case study shows that the proposed HCS constraint can be well coupled into the model to ensure power transmission security. The peak-valley difference in dry and flood season reduced by 37% and 21%, respectively, which indicates that the model can make full use of the flexibility of hydropower to achieve a satisfactory peak-shaving result.

1. Introduction

In China, the hydropower resource are mainly distributed in the southwestern region, while the load center is located in the eastern coastal area [1]. To address the geographical mismatch between hydropower generation and load demand, many long-distance power transmission projects have been constructed [2], among which HVDC transmission tie lines occupied the majority for their economy and safety in long-distance and large-capacity power transmission [3,4]. Moreover, the increasing load demand and peak-valley difference pose higher peak-shaving pressure for power grids in recent years [5,6]. Hydropower, characterized by large peak amplitudes, rapid startup/shutdown of units and high ramping rates, is regarded as an ideal power supply for deep peak regulation [7,8]. Thus, to fully use the flexibility of hydropower to reduce the peak-valley difference of power grids, many huge hydropower stations in southwest China are sending power to the load centers through HVDC transmission lines. For example, the Three Gorges (TG), with the largest installed capacity in the world, transmits

power to ECPG and CSPG through SG HVDC line; Xiangjiaba (XJB), with the 4th largest installed capacity in the world, sends power to ECPG through FF UHVDC line; Xiaowan (XW), with the 25th largest installed capacity in the world, sends power to CSPG and YNPG through CS UHVDC line. Table 1 lists some hydropower stations with the top installed capacity in the world and their corresponding transmission lines. Peak-shaving operation for power grids through long-distance hydropower transmission by HVDC tie lines is widespread and important.

The modeling of hydropower peak-shaving operation through HVDC power transmission has attracted many scholars. Shen et al. [9] coordinated the operations of UHVDC hydropower and conventional hydropower for regional power grids. Cao et al. [10] studied the monthly inter-regional hydropower scheduling considering HVDC constraints. Xu et al. [11] proposed a multi-objective optimal scheduling strategy for wind power, solar power and pumped storage hydropower in VSC-HVDC grid. Yuan et al. [12] studied cross-regional integrated transmission of wind power and pumped-storage hydropower. However, the existing studies mainly focused on a single hydropower station,

* Corresponding author.

E-mail addresses: shengliliao@dlut.edu.cn (S. Liao), yhl_dlut@163.com (H. Yang), benxiliu@dlut.edu.cn (B. Liu), zhaohy@mail.dlut.edu.cn (H. Zhao), dlut_huanliu@foxmail.com (H. Liu), mxy0324@mail.dlut.edu.cn (X. Ma), wuhj@csg.cn (H. Wu).

Nomenclature					
A. Acronyms					
CS	Chusui UHVDC tie lines	$P_{g,t}^{\text{in}}$	power input of power grid g at period t		
CSPG	China South Power Grid	$P_{i,t}^{\text{loc}}$	power output of hydropower station i at period t		
ECPG	East China Power Grid	$P_{i,t}^{\text{ext}}$	transmitted to local power grid		
GDPG	Guangdong Power Grid	P_i^{ramp}	power output of hydropower station i at period t		
HCS	HVDC channel shared	\bar{P}_i	transmitted to external power grid		
HVAC	high voltage alternating current	\underline{P}_i	maximum allowable power output of hydropower station i		
HVDC	high voltage direct current	Q_i^{gen}	minimum allowable power output of hydropower station i		
MAE	mean absolute error	P_i^{gen}	maximum power output ramping of hydropower station i		
MILP	mixed integer liner programming	$Q_{i,t}$	generation discharge of hydropower station i at period t		
MSE	mean square error	\bar{Q}_i	maximum allowable generation discharge of hydropower station i		
PQ	Puqiao UHVDC tie lines	\underline{Q}_i	minimum allowable generation discharge of hydropower station i		
UHVDC	ultra-high voltage direct current	$Q_{i,t}^{\text{in}}$	total inflow of hydropower station i at period t		
YNPG	Yunnan Power Grid	$Q_{i,t}^{\text{out}}$	total outflow of hydropower station i at period t		
B. Sets and indices		$q_{i,t}$	natural inflow of hydropower station i at period t		
G, g	set and index of power grids	R_e	electricity receiving ratio of local and external power grid		
I, i	set and index of hydropower stations	$V_{i,t}$	water storage of hydropower station i at period t		
II, j	set and index of hydropower stations that send power by tie line l	\bar{V}_i	maximum water storage of hydropower station i		
L, l	set and index of HVDC tie lines	\underline{V}_i	minimum water storage of hydropower station i		
T, t	set and index of time periods	$Z_{i,t}$	forebay water level of hydropower station i at period t		
C. Parameters and variables		\bar{Z}_i	maximum forebay water level of hydropower station i		
$D_{g,t}$	residual load in power grid g at period t	\underline{Z}_i	minimum forebay water level of hydropower station i		
D_g^{mae}	mean absolute error of residual load in power grid g	$Z_{i,t}^{\text{tail}}$	tail water level of hydropower station i at period t		
$H_{i,t}$	net water head of hydropower station i at period t	Z_i^{initial}	initial forebay water level of hydropower station i		
$h_{i,t}^{\text{loss}}$	water head loss of hydropower station i at period t	Z_i^{final}	final forebay water level of hydropower station i		
$L_{g,t}^{\text{PG}}$	original load of power grid g at period t	φ_i	minimum power output duration of hydropower station i		
$L_{l,t}^{\text{DC}}$	load on HVDC line l at period t	ω_g	weight factor of power grid g in objective function		
\bar{L}_l^{DC}	maximum allowable load on HVDC line l	D. Functions			
$\underline{L}_l^{\text{DC}}$	minimum allowable load on HVDC line l	$f_{\text{NQH}}(\cdot, \cdot)$	function of power output, generation discharge and net water head		
ΔL_l^{DC}	maximum load change between adjacent periods of HVDC line l	$f_{\text{zQ}}(\cdot)$	function of tail water level and total outflow		
$P_{i,t}$	power output of hydropower station i at period t	$f_{\text{zv}}(\cdot)$	function of forebay water level and water storage		

Table 1
Huge hydropower plants in China and corresponding transmission lines.

Hydropower station	Installed capacity (MW)	Installed world ranking	HVDC/UHVDC transmission line	Line capacity (MW)	Receiving power grids
TG	22500	1st	SG HVDC	3000	ECPG, CSPG
XLD	13860	4th	NC HVDC	6400	ECPG, CSPG
XJB	6400	9th	FF UHVDC	6400	ECPG
NZD	5850	15th	PQ UHVDC	5000	CSPG, YNPG
XW	4200	25th	CS UHVDC	5000	CSPG, YNPG

without considering the hydraulic interaction between cascade hydropower stations. In this paper, a daily peak-shaving model for cross-basin cascade hydropower stations serving multiple power grids via HVDC transmission lines is established, in which we deal with the difficulties from complicated cascade hydraulic connections, coordination of cross-basin hydropower stations, complex HVDC constraints and load demand contradiction among multiple receiving power grids.

When multiple hydropower stations transmit power by sharing one

HVDC channel, the sending-end power grid must be limited by the constraints on power transmission network. However, there are few studies on the constraints of HVDC power transmission network in hydropower scheduling. Shen et al. [13] considered simple HVDC line constraints such as the maximum and minimum load limits and load fluctuation limit. Su et al. [14] first proposed the stair-like HVDC constraint to avoid frequent conversion of the load on HVDC tie lines. Liu et al. [15] added the maximum daily power regulation times in addition to the stair-like constraint to prevent frequent fluctuations of the load on HVDC tie lines. Xu et al. [16] considered conditional sections in the inter-regional HVDC tie-line generation and transmission system. These studies ensured the safety of HVDC tie line, but they only paid attention to the constraints on HVDC tie lines, ignoring the coupling between hydropower stations and the HVDC channel. In fact, one HVDC power transmission channel is usually shared by multiple hydropower stations. For example, CS UHVDC channel is shared by XW and JAQ, PQ UHVDC channel is shared by NZD and JH. When multiple hydropower stations share one HVDC channel, they will compete for the transmission capacity. Without appropriate constraints, there will be a high risk on the power transmission network, which can even threaten the stability of entire power grid [17,18]. In this paper, for multiple cross-basin or cascade hydropower stations that share one power transmission channel, an HVDC channel shared (HCS) constraint is presented, which restrict the connection between the hydropower stations and the HVDC

transmission channel. Because it hard to be modeled, the HCS constraint is restructured by the set-calculation method for simple and mathematical expression, then integrated into the multiple power grids' short-term peak-shaving model.

Multiple power grids daily peak-shaving of cascade hydropower stations via HVDC power transmission is essentially a day-ahead hydropower generation scheduling (DHGS) problem. Many methods have been introduced to solve the DHGS problem in the recent years, including dynamic programming (DP) and its improved methods [19–21], the mathematical programming methods such as nonlinear programming (NLP) [22,23] and linear programming (LP) [24], and the intelligent algorithms such as the genetic algorithm (GA) [25,26], particle swarm optimization (PSO) [27] and differential evolution (DE) algorithm [28]. However, these methods present different difficulties in solving the above problem in this paper. DP and its improved methods have the “Curse of dimensionality” in multiple hydropower-cascades scheduling; NLP needs high computational cost due to its convex constraints; LP will lead to large error in short-term scheduling; The intelligent algorithms cannot guarantee the global optimum within finite iterations. In comparison to the above programming methods, mixed integer linear programming (MILP) is increasingly applied in the DHGS problem in recent years due to its mature mathematical theory in schedule modeling and high efficiency in model solution with a large scale variables [29–32], which is exactly suitable for the modeling of the complicated problem in this paper that involves complex hydraulic connection between inter-basin cascade hydropower stations, large scale variables in short-term scheduling and complicated nonlinear constraints. To transform the proposed NLP model in this paper to an MILP model, the nonlinear items need to be linearized. The HCS constraint in this study is highly nonlinear, especially. The Big-M method, with high efficiency and flexibility in handling massive inequality constraints, is adopted for the linearization of the HCS constraint. Moreover, the nonlinear hydraulic constraints are also linearized. Using commercial solvers such as CPLEX and GUROBI, the MILP model is expected to be solved within a satisfactory CPU time.

This paper focuses on modeling of the HCS constraint, which is restructured and linearized to form an MILP model. The remainder of this paper is organized as follows: Section 2 introduces the engineering background of the study. Section 3 builds the mathematical model integrating the HCS constraint. Section 4 describes the restructuring of the HCS constraint, linearization transformation of the model, and the whole solution framework. Section 5 shows the case study results of the dry and flood seasons, the sensitivity analysis of the electricity receiving ratio and the influence evaluation of the HCS constraint. Section 6 outlines the conclusion.

2. Engineering background

Yunnan Province, located in southwest China with several large rivers of great elevation differences, has more than 20% of the total installed capacity of hydropower in China. With the implementation of “West to East Power Transmission Project”, the installed capacity in Yunnan surged from 28,420 MW in 2011 to 78,198 MW in 2021, mainly distributed in the basins of Lancang river and Jinsha river. Moreover, the power generation of Yunnan Province in 2021 reaches 343.4 GWh, 38% of which is transmitted to GDPG through HVDC tie lines. HVDC power transmission has become the main way for the hydropower consumption in Yunnan Province.

This paper takes an actual power transmission system in southern China including six hydropower plants locating in two basins, two power grids of GPG and YNPG, and two HVDC tie lines of CS and PQ as a study case. The six hydropower stations are XW, MW, DCS, NZD, JH and JAQ. Both CS and PQ are ±800 kV UHVDC lines with transmission capacity of 5000 MW. The power transmission topology is shown in Fig. 1.

XW and JAQ send hydropower to GPG through the CS UHVDC tie line, which means they must share the same HVDC channel. To ensure the security of HVDC channel shared transmission, the HCS constraint need to be considered. The HCS constraint among the XW, JAQ and CS UHVDC is shown in Table 2, which means when the difference (P_{remain}) between the load on the CS UHVDC line (P_{CS}) and the power output of JAQ (P_{JAQ}) is located in a certain interval, the power output of XW (P_{XW}) must satisfy the corresponding limit in the meanwhile. Larger P_{remain} corresponding to higher power shortage, which need more power output from XW (e.g. Segment 1). While the negative value of P_{remain} means that the load demand of CS HVDC line can be fully satisfied by the power output of JAQ, which requires a lower level of XW's power output to prevent overload on the HVDC line (e.g. Segment 8).

Table 2
The HCS constraint between XW, JAQ and CS.

Segment	P_{remain}/MW	P_{XW}/MW
1	$4500 < P \leq 5000$	$3000 \leq P \leq 4200$
2	$4000 < P \leq 4500$	$2200 \leq P \leq 4200$
3	$3500 < P \leq 4000$	$1400 \leq P \leq 4200$
4	$3100 < P \leq 3500$	$650 \leq P \leq 4200$
5	$-600 < P \leq 3100$	$0 \leq P \leq 4200$
6	$-1200 < P \leq -600$	$0 \leq P \leq 3100$
7	$-1800 < P \leq -1200$	$0 \leq P \leq 2200$
8	$-2400 < P \leq -1800$	$0 \leq P \leq 1250$

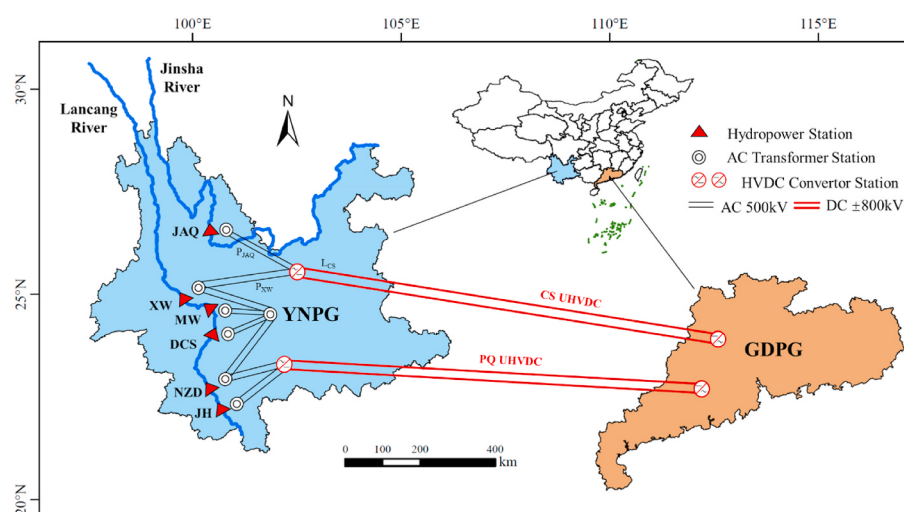


Fig. 1. Power transmission topology in YNPG and GPG.

3. Mathematical model

3.1. Objection function

Short-term hydropower peak-shaving operation aims to formulate a day-ahead generation plan for hydropower stations to minimizing the fluctuation of the residual load of power grids under various complicated constraints. The minimum mean square error (MSE) of residual load is commonly used as the objective function of hydropower short-term peak-shaving operation, but the quadratic term in which cannot be linearized. As the replacement form, the minimum mean absolute error (MAE) of residual load is used as the objective function in this paper (Eqs. (1)–(3)).

$$\min F = \sum_{g \in G} \omega_g D_g^{\text{mae}} \quad (1)$$

$$D_g^{\text{mae}} = \frac{1}{T} \sum_{t=1}^T \left| D_{g,t} - \frac{1}{T} \sum_{t=1}^T D_{g,t} \right| \quad (2)$$

$$D_{g,t} = L_{g,t} - P_{g,t}^{\text{in}}$$

3.2. Hydraulic and electric constraints

1. Electricity receiving ratio of local and external power grid

$$R_e = E^{\text{loc}} / E^{\text{ext}} \quad (4)$$

2. Power output division of hydropower stations

$$P_{i,t} = P_{i,t}^{\text{loc}} + P_{i,t}^{\text{ext}} \quad (5)$$

3. Forebay water level limit

$$\underline{Z}_i \leq Z_{i,t} \leq \bar{Z}_i \quad (6)$$

4. Power output limit

$$\underline{P}_i \leq P_{i,t} \leq \bar{P}_i \quad (7)$$

5. Continuity balance equation

$$V_{i,t} = V_{i,t-1} + (Q_{in,i,t} - Q_{out,i,t}) \Delta t \times 3600 \quad (8)$$

6. Total inflow equation

$$Q_{in,i,t} = q_{i,t} + Q_{out,i-1,t} \quad (9)$$

7. Generation discharge limit

$$\underline{Q}_i \leq Q_{i,t} \leq \bar{Q}_i \quad (10)$$

8. Total outflow limit

$$\underline{Q}_{out,i} \leq Q_{out,i,t} \leq \bar{Q}_{out,i} \quad (11)$$

9. Net water head equation

$$H_{i,t} = (Z_{i,t-1} + Z_{i,t}) / 2 - Z_{i,t}^{\text{tail}} - h_{\text{loss},i,t} \quad (12)$$

10. Power output ramping constraint

$$|P_{i,t+1} - P_{i,t}| \leq P_i^{\text{ramp}} \quad (13)$$

11. Minimum power output duration constraint

$$(P_{i,t+1} - P_{i,t})(P_{i,t+\alpha+1} - P_{i,t+\alpha}) \geq 0, \alpha = 1, 2, \dots, \varphi_i - 1; t = 1, 2, \dots, T - \varphi_i \quad (14)$$

12. Function between power output, generation discharge and net water head

$$P_{i,t} = f_{i,\text{NQH}}(Q_{i,t}, H_{i,t}) \quad (15)$$

13. Function between forebay water level and storage

$$V_{i,t} = f_{i,\text{ZV}}(Z_{i,t}) \quad (16)$$

14. Function between tail water level and total outflow

$$Z_{i,t}^{\text{tail}} = f_{i,\text{ZQ}}(Q_{out,i,t}) \quad (17)$$

15. Initial and final forebay water level limits

$$\begin{cases} Z_{i,0} = Z_i^{\text{initial}} \\ Z_{i,T} = Z_i^{\text{final}} \end{cases} \quad (18)$$

3.3. HVDC constraints

To meet the demand of hydropower consumption and peak-shaving demands of receiving power grids, and ensure the stability of the power transmission network, the following additional constraints need to be considered.

1. Load composition of HVDC tie lines

$$L_{l,t}^{\text{DC}} = \sum_{i \in l} P_{i,t}^{\text{ext}} \quad (19)$$

2. Maximum and minimum load limit of tie lines

$$\underline{L}_l^{\text{DC}} \leq L_{l,t}^{\text{DC}} \leq \bar{L}_l^{\text{DC}} \quad (20)$$

3. Load variation constraint of tie lines

$$|L_{l,t+1}^{\text{DC}} - L_{l,t}^{\text{DC}}| \leq \Delta L_l^{\text{DC}} \quad (21)$$

4. HVDC channel shared (HCS) constraint

To generalize the constraint in Table 2, we propose the generalized HCS constraint, which can be applied in each case of multiple hydropower stations sharing one HVDC channel:

$$b_n \leq P_{i^0,t} \leq \bar{b}_n, \text{ if } : \underline{a}_n \leq L_{l,t}^{\text{DC}} - \sum_{j \neq i^0} P_{j,t}^{\text{DC}} \leq \bar{a}_n \quad (22)$$

In which when the difference between the HVDC line load ($L_{l,t}^{\text{DC}}$) and the total power output of the remaining hydropower plants ($\sum_{i \neq i^0} P_{i,t}$) is in any possible range $[\underline{a}_n, \bar{a}_n]$, the power output of the main power source ($P_{i^0,t}$) must fall in the corresponding range $[b_n, \bar{b}_n]$. i^0 is the main hydropower source that sends power to HVDC line l .

4. Solution techniques

In this section, the restructuring method of single power grid and multiple power grids is suggested respectively, and some other methods

are introduced to linearize the nonlinear items in the model especially for the restructured HCS constraint.

4.1. Single power grid restructuring of the HCS constraint

The HCS constraint in Eq. (22) cannot be directly modeled and solved due to the “if statement”. To integrate the HCS constraint into a single power grid, the following methods based on set-calculation are proposed.

In the case of power transmission to single power grid, the hydropower plants only send power to a single external power grid by sharing one HVDC transmission line, where the total power output of the hydropower stations is equal to the HVDC load.

$$L_{l,t}^{\text{DC}} = \sum_{i \in I_l} P_{i,t} \quad (23)$$

In Eq. (22), let:

$$\begin{cases} S_n^a = \left[\underline{a}_n, \bar{a}_n \right] \\ S_n^b = \left[\underline{b}_n, \bar{b}_n \right] \end{cases} \quad (24)$$

where S_n^a and S_n^b are limits of main hydropower station's power output in the HCS constraint.

Taking two hydropower stations as an example, Eq. (22) can be expressed as follows:

$$P_{f_l^0,t} \in S_n^a \cap S_n^b \quad (25)$$

Let:

$$\begin{cases} S_n = S_n^a \cap S_n^b \\ S = S_1 \cup S_2 \cup \dots \cup S_n \cup \dots \cup S_N = \bigcup_{n=1}^N S_n \end{cases} \quad (26)$$

where S_n is the intersection of S_n^a and S_n^b , and S is the union of S_n .

Then, the HCS constraint shown in Eq. (23) is transferred to:

$$P_{f_l^0,t} \in S \quad (27)$$

Therefore, in the power transmission to single power grid, Eq. (22) is equivalent to Eq. (27), where S is obtained by a set operation, which is known in advance. Even so, S is discontinuous, so the expression is nonlinear.

4.2. Multiple power grids restructuring of the HCS constraint

In addition to sending power to the external power grid, most of the large hydropower stations in southwest China also send power to the local power grid. When the hydropower stations send power output to multiple power grids, Eq. (23) is no longer applicable, so the above restructuring method for a single power grid is also inapplicable. The restructuring method of the HCS constraint in this case is proposed as follows:

In power transmission to multiple power grids, we define $P_{i,t}^{\text{loc}}$ and $P_{i,t}^{\text{ext}}$ as the power output of station i that are sent to the local and external power grid, respectively:

$$P_{i,t} = P_{i,t}^{\text{loc}} + P_{i,t}^{\text{ext}} \quad (28)$$

Thus, the load on HVDC line l are only consisted by the hydropower stations' power output that transmits to the external power grid, which is different from Eq. (23):

$$L_{l,t}^{\text{DC}} = \sum_{i \in I_l} P_{i,t}^{\text{ext}} \quad (29)$$

In power transmission to multiple power grids, define the power

output distribution proportion $\alpha_{i,t}$ between the local power grid and the external power grid:

$$\alpha_{i,t} = P_{i,t}^{\text{loc}} / P_{i,t}^{\text{ext}} \quad (30)$$

Then Eq. (28) can be expressed as:

$$P_{i,t} = (\alpha_{i,t} + 1) P_{i,t}^{\text{ext}} \quad (31)$$

Taking two hydropower stations as an example, we use $P_{1,t}$ and $P_{2,t}$ to represent the main and the another hydropower source, respectively. Then Eq. (22) can be transformed into:

$$\begin{cases} \underline{a}_n \leq L_{l,t}^{\text{DC}} - P_{2,t} \leq \bar{a}_n \\ \underline{b}_n \leq P_{1,t} \leq \bar{b}_n, n \in \{1, 2, \dots\} \end{cases} \quad (32)$$

Transform Eq. (32) according to Eqs. 28–31:

$$\begin{aligned} L_{l,t}^{\text{DC}} - P_{2,t} &= \left(P_{1,t}^{\text{ext}} + P_{2,t}^{\text{ext}} \right) - \left(P_{2,t}^{\text{loc}} + P_{2,t}^{\text{ext}} \right) \\ &= P_{1,t}^{\text{ext}} - \alpha_{2,t} P_{2,t}^{\text{ext}} \\ &= P_{1,t}^{\text{ext}} - \alpha_{2,t} \left(L_{l,t}^{\text{DC}} - P_{1,t}^{\text{ext}} \right) \\ &= (1 + \alpha_{2,t}) P_{1,t}^{\text{ext}} - \alpha_{2,t} L_{l,t}^{\text{DC}} \\ &= \frac{1 + \alpha_{2,t} P_{1,t} - \alpha_{2,t} L_{l,t}^{\text{DC}}}{1 + \alpha_{1,t}} \end{aligned} \quad (33)$$

Then, Eq. (32) can be expressed as:

$$\begin{cases} \underline{a}_n \leq \frac{1 + \alpha_{2,t} P_{1,t} - \alpha_{2,t} L_{l,t}^{\text{DC}}}{1 + \alpha_{1,t}} - \alpha_{2,t} L_{l,t}^{\text{DC}} \leq \bar{a}_n \\ \underline{b}_n \leq P_{1,t} \leq \bar{b}_n, n \in \{1, 2, \dots\} \end{cases} \quad (34)$$

In which $P_{2,t}$ is eliminated, therefore:

$$\begin{cases} \frac{(1 + \alpha_{1,t})(\underline{a}_n + \alpha_{2,t} L_{l,t}^{\text{DC}})}{(1 + \alpha_{2,t})} \leq P_{1,t} \leq \frac{(1 + \alpha_{1,t})(\bar{a}_n + \alpha_{2,t} L_{l,t}^{\text{DC}})}{(1 + \alpha_{2,t})} \\ \underline{b}_n \leq P_{1,t} \leq \bar{b}_n, n \in \{1, 2, \dots\} \end{cases} \quad (35)$$

Let:

$$\begin{cases} S_{n,t}^a = \left[\frac{(1 + \alpha_{1,t})(\underline{a}_n + \alpha_{2,t} L_{l,t}^{\text{DC}})}{(1 + \alpha_{2,t})}, \frac{(1 + \alpha_{1,t})(\bar{a}_n + \alpha_{2,t} L_{l,t}^{\text{DC}})}{(1 + \alpha_{2,t})} \right] \\ S_{n,t}^b = \left[\underline{b}_n, \bar{b}_n \right] \end{cases} \quad (36)$$

$$S_{n,t} = S_{n,t}^a \cap S_{n,t}^b = \left[\underline{S}_{n,t}, \bar{S}_{n,t} \right] \quad (37)$$

According to the properties of convex sets, it can be guaranteed that $S_{n,t}$ is still a convex set, where:

$$\begin{cases} \overline{S_{n,t}} = \min \left\{ \overline{S_{n,t}^a}, \overline{S_{n,t}^b} \right\} \\ \underline{S_{n,t}} = \max \left\{ \underline{S_{n,t}^a}, \underline{S_{n,t}^b} \right\} \end{cases} \quad (38)$$

Let:

$$S_t = S_{1,t} \cup S_{2,t} \cup \dots \cup S_{N,t} = \bigcup_{n=1}^N S_{n,t} \quad (39)$$

Finally, Eq. (32) is transformed to:

$$P_{1,t} \in S_t \quad (40)$$

Thus, in the power transmission to multiple power grids, Eq. (22) is equivalent to Eq. (40), the complex HCS constraint is transformed to a set constraint, which can be modeled and efficiently solved. However,

unlike the power transmission to single power grid, $\alpha_{1,t}, \alpha_{2,t}$ in Eq. (36) are unknown and must be optimized in the model. Moreover, S_t is nonconvex, and the division in Eq. (35) turns the HCS constraint into a nonlinear item, which must be linearized.

4.3. Linearization of the model

The proposed model contains both linear constraints and nonlinear constraints. To transform the nonlinear programming (NLP) into the MILP, the nonlinear items, include the objective function, nonlinear hydraulic constraints and nonlinear HVDC constraints, are addressed by proper linearization techniques. The restructured HCS constraint is linearized by the *Big-M* method in this paper.

1. Linearization of the HCS constraint

The restructured HCS constraint in Eq. (40) is nonlinear because it cannot be guaranteed that set S_t is convex, and $S_{n,t}$ may not exist (for example, $S_{n,t} = [0, -100]$). The *Big-M* method, with high efficiency and flexibility in handling massive inequality constraints, is adopted in this paper for the linearization of the HCS constraint:

$$\left\{ \begin{array}{l} \underline{S}_{n,t} - M(1 - \lambda_n^t) \leq P_{1,t} \leq \overline{S}_{n,t} + M(1 - \lambda_n^t) \\ \sum_{n=1}^N \lambda_n^t = 1, \quad \lambda_n^t = \{0, 1\}, \quad n \in \{1, 2, \dots\} \end{array} \right. \quad (41)$$

where M is a sufficiently large number, λ_n^t is a binary indicator, $\lambda_n^t = 1$ means that $P_{1,t}$ falls into the interval $S_{n,t} = [\underline{S}_{n,t}, \overline{S}_{n,t}]$. Furthermore, $\alpha_{1,t}, \alpha_{2,t}$ in Eq. (35) are uncertain variables to linearize the HCS constraint, it is defined that $\alpha_{1,t} = \alpha_{2,t} = \alpha_t$ in the model optimization.

2. Linearization of the objective function

The absolute value in the objective function (Eq. (2)) is linearized as follow:

$$\left\{ \begin{array}{l} D_g^{\max} = \frac{1}{T} \sum_{t=1}^T D_{g,t}^{\text{abs}} \\ D_{g,t}^{\text{abs}} \geq D_{g,t} - \frac{1}{T} \sum_{t=1}^T D_{g,t} \\ D_{g,t}^{\text{abs}} \geq - \left(D_{g,t} - \frac{1}{T} \sum_{t=1}^T D_{g,t} \right) \end{array} \right. \quad (42)$$

Similarly, the absolute value in power output ramping constraints (Eq. (13)) and HVDC load variation constraint (Eq. (21)) are linearized by the same method.

3. Linearization of power output duration constraints

The quadratic term in the minimum power output duration constraints (Eq. (14)) is linearized as follows:

$$\left\{ \begin{array}{l} P_{i,t+1} - P_{i,t} = P_{i,t}^{\text{up}} - P_{i,t}^{\text{down}} \\ U_{i,t}^{\text{up}} = \sum_{\tau=t}^{t+\varphi_i-1} P_{i,\tau}^{\text{up}} \\ U_{i,t}^{\text{down}} = \sum_{\tau=t}^{t+\varphi_i-1} P_{i,\tau}^{\text{down}} \\ \text{SOS1}\left(U_{i,t}^{\text{up}}, U_{i,t}^{\text{down}}\right) \end{array} \right. \quad (43)$$

where, $P_{i,t}^{\text{up}}$ and $P_{i,t}^{\text{down}}$ are the ramping up or ramping down of hydro-

power station i at period t , respectively; $U_{i,t}^{\text{up}}$ and $U_{i,t}^{\text{down}}$ are the summations of $P_{i,t}^{\text{up}}$ and $P_{i,t}^{\text{down}}$ from period t to the later φ_i periods, respectively, the SOS1 is the first type of special ordered sets constraint, which indicates that the power output cannot simultaneously increase and decrease at the same period.

4. Piecewise linear interpolation (PLI) of the relationship functions

The function between forebay water level and storage, tail water level and total outflow are usually fitted by quartic or quadratic curves in nonlinear model. While in MILP model, the PLI is usually adopted to linearize these relationship functions by introducing integer variables. Taking the function between forebay water level and storage as an example, the PLI is introduced as follows:

$$\left\{ \begin{array}{l} \sum_{w=0}^W \lambda_w = 1 \\ \sum_{w=0}^W \lambda_w Z_w^{\text{piece}} = Z \\ \sum_{w=0}^W \lambda_w V_w^{\text{piece}} = V \\ \text{SOS2}(\lambda_0, \lambda_1, \dots, \lambda_W) \end{array} \right. \quad (44)$$

where Z_w^{piece} and V_w^{piece} are the forebay water level and storage of piecewise point w , respectively, and λ_w is the corresponding binary variable. The SOS2 is the second type of special ordered sets constraint, which limits that at most two adjacent λ_w are allowed to be nonzero.

The PLI of the relationship functions between tail water level and total outflow is identical to the abovementioned, the nonlinear NHQ relationship function is linearized by the triangular mesh linear interpolation method, which is three-dimensional compared with the PLI method, the similar linearization methods will not be repeated.

4.4. Solution framework

The solution framework includes three main sections, which is shown in Fig. 2. In model construction, the multiple power grids daily peak-shaving operation model considering HVDC constraints is built by three parts. Model solution includes the conventional hydropower scheduling problem and the HVDC hydropower scheduling problem. While the linearization strategy and the restructuring strategy are introduced to reduce the solution time. When the optimization solution reaches the termination condition, we stop the optimization and output the optimal result.

5. Result analysis

Applying the MILP model constructed in Part 3 to the engineering background in Part 2, this paper takes the six hydropower stations as operation objects, considers the HCS constraint among XW, JAQ and the CS HVDC tie line, attempts to formulate an hourly power generation and transmission plan to shave the daily load peak of GDPG and YNPG. First, the peak-shaving effects of power grids in the dry and flood season are analyzed according to the optimization result. Then, the influence of different electricity receiving ratios on the peak-shaving effect is analyzed. Finally, the sensitivity of the HCS constraint is evaluated. The model is written by Python 3.8 and solved by the optimization solver GUROBI 9.2.

5.1. Analysis of the optimal result in dry season

The natural inflows of the hydropower stations of a representative day in the dry season are given. The daily initial and final forebay water levels of the reservoirs are pre-determined according to the actual

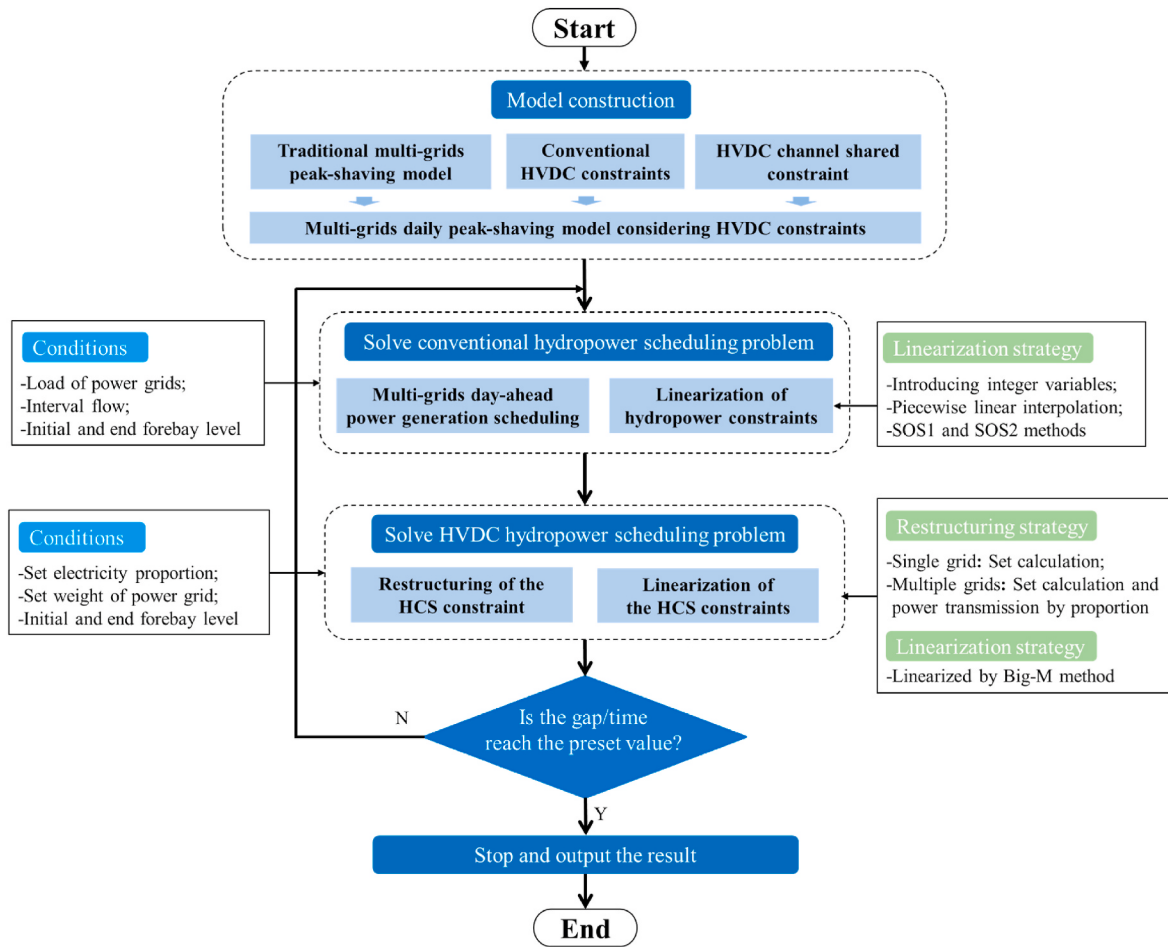


Fig. 2. Solution framework.

operation data. The water surplus is not allowed. Set $R_e = 1/2$, and $\omega_{YNPG} = \omega_{GDPG} = 1$.

Table 3 and **Fig. 3(a)-(b)** show the optimal peak-shaving result of each power grid in the dry season. **Table 3** lists the electricity reception and peak-valley difference descent of GDPG, YNPG and the total load. The result shows that compared with the original loads, the peak-valley differences of the residual loads in GDPG and YNPG are reduced by 31% and 55%, respectively, and the peak-valley difference of the total load is reduced by 37%. Due to both the load level and peak-valley difference are far less than that in GDPG, the peak-shaving effect of YNPG is more satisfactory.

Fig. 3(c) is the accumulation diagram of the hydropower stations, where each hydropower station shows an obvious peak-shaving characteristic to satisfy the peak-shaving demand of the power grids. **Fig. 3(d)** is the optimal load processes of HVDC lines in the dry season, in which the power output in valley load periods maintains at the lowest level of 500 MW, while that in peak load periods rapidly climbs and

maintains at the maximum load level of 5000 MW. Since both CS and PQ transmit electricity to GDPG, their load processes have similar characteristic.

5.2. Analysis of the optimal result in flood season

The natural inflows of the hydropower stations of a representative day in the flood season are given. The daily initial and final forebay water levels of the reservoirs are pre-determined according to the actual operation data. The water surplus is not allowed. Set $R_e = 1/2$, and $\omega_{YNPG} = \omega_{GDPG} = 1$.

Table 4 and **Fig. 4(a)-(b)** show the peak-shaving result of the power grids in the flood season. **Table 4** lists that the total electricity received by the power grids in the flood season reaches 326.4 GWh, which is approximately 60% more than that in the dry season. Compared with that in the dry season, the peak-valley difference descent of GDPG in the flood season decreases to 17%, which is attributed to the transmission capacity of the HVDC tie lines reaching to the maximum in the dry season. In contrast, the peak-valley difference descent of YNPG increases to 66% due to the peak regulation of the local power grid is not limited by the HVDC transmission capacity. The peak-valley difference descent of the total load decreases to 21%, which is obviously dominated by GDPG. In **Fig. 4(c)**, although the peak-shaving effect of the hydropower stations decreases due to more natural inflow in the flood season, the total load curve still maintains a peak-shaving characteristic, XW, DCS and NZD are the three main peaking power sources, and the others bear the base load.

Fig. 4(d) shows the optimal load process of HVDC transmission lines in the flood season, in which the loads on the tie lines reach the

Table 3
Peak-shaving result of power grids in the dry season.

Items	GDPG	YNPG	Total load
Electricity received/GWh	125.4	62.7	188.1
Original load/MW	Peak of original load	81000	23732
	Valley of original load	52050	16185
	Peak-valley difference	28950	7547
Residual load/MW	Peak of residual load	71000	19027
	Valley of residual load	51050	15595
	Peak-valley difference	19950	3432
Peak-valley difference descent	31%	55%	37%

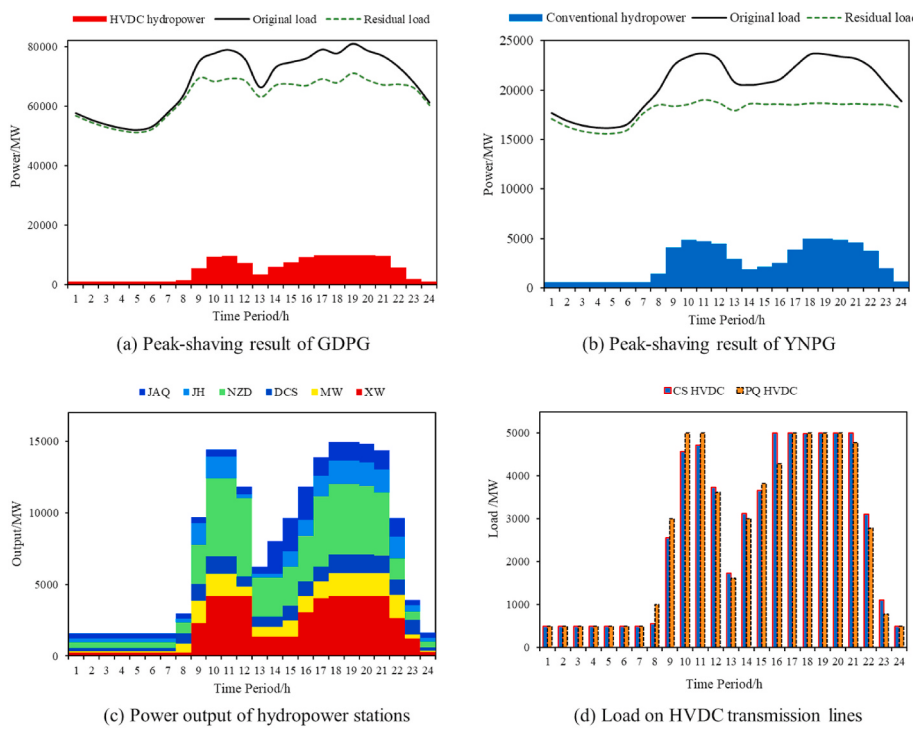


Fig. 3. Optimization result in the dry season.

Table 4
Peak-shaving result of power grids in the flood season.

Items	GDPG	YNPG	Total load
Electricity received/GWh	217.6	108.8	326.4
Original load/MW	Peak of residual load 120405	26047	144179
	Valley of original load 83815	19696	103859
	Peak-valley difference 36590	6351	40320
Residual load/MW	Peak of residual load 110405	19526	129163
	Valley of original load 79961	17377	97438
	Peak-valley difference 30444	2149	31725
Peak-valley difference descent	17%	66%	21%

maximum level in most periods of the day. Table 5 compares the optimal load results of the HVDC lines in the dry and flood season. The results indicate that the electricity transmission of the tie lines in the flood season sharply increases compared with that in the dry season. Due to the limit of maximum transmission capacity, the load rates of CS line and PQ line significantly increase from 52% to 52% in dry season to 87% and 94% in flood season, respectively.

5.3. Sensitivity analysis of electricity receiving ratio

When the scheduling department make the day-ahead peak-shaving operation plan for multiple power grids, they usually give the total electricity demand and electricity receiving ratio of each power grid. When the total power generation is given, the peak-shaving effect of each power grid is sensitive to the electricity receiving ratios, which is used to flexibly adjust the power transmission and balance the peak-shaving demand for each power grid.

This part takes one representative day in the dry season as the operation period, different R_e values are used to transmit electricity to YNPG and GPGD. The selected R_e values are 1/1, 1/2, 1/3 and 1/4, respectively.

Table 6 and Fig. 5(a) compare the influence from different electricity receiving ratios on the optimal operation result. It can be seen in Table 6 that YNPG and GPGD basically follow the trend of more electricity

reception leading to a better peak-shaving effect. However, when $R_e = 1/4$, the opposite trend appears, which possibly because the power output of hydropower stations reach to maximum level during the peak load periods, which implies that they have no more capacity to shave the peak load. Fig. 5(b) indicates that when more electricity sending to GPGD, the load level on HVDC tie lines increases because the tie lines only transmit power to GPGD.

5.4. Influence analysis of the HCS constraint

This part takes the two conditions, before and after imposing the HCS constraint separately, to evaluate the influence of the HCS constraint. The influence of the HCS constraint is assessed by comparing the XW power output results. We take the flood season as an example and set $R_e = 1/2$.

The shadow areas in Fig. 6 are the forbidden operation range of P_{xw} , which is decided by the HCS constraint. The three dotted line circle A, B and C in Fig. 6(a) shows that without considering the HCS constraint, the curve of P_{xw} will pass through the forbidden operation range in three periods (1st, 9th and 22nd). While after considering the HCS constraint to the model in Fig. 6(b), the three new points in the same periods, A', B' and C', avoid the forbidden range. For example, before imposing the HCS constraint, P_{xw} is 2600 MW (point A), which is beyond the limit of 2250 MW, while after imposing the HCS constraint, it declines to 2200 MW (point A'), which falls in the allowed operation range. The result indicates that the HCS constraint can effectively limit the power output of the hydropower stations that transmits power to HVDC tie lines to ensure the stable operation of the power grid.

6. Conclusion

This study focused on restructuring and modeling of the HCS constraint to tackle the short-term hydropower peak-saving operation problem coupling the long-distance hydropower transmission via HVDC tie lines. A daily peak-shaving model for cascade hydropower serving multiple power grids was established, in which the HCS constraint was considered. Six huge hydropower stations, two HVDC tie lines and two

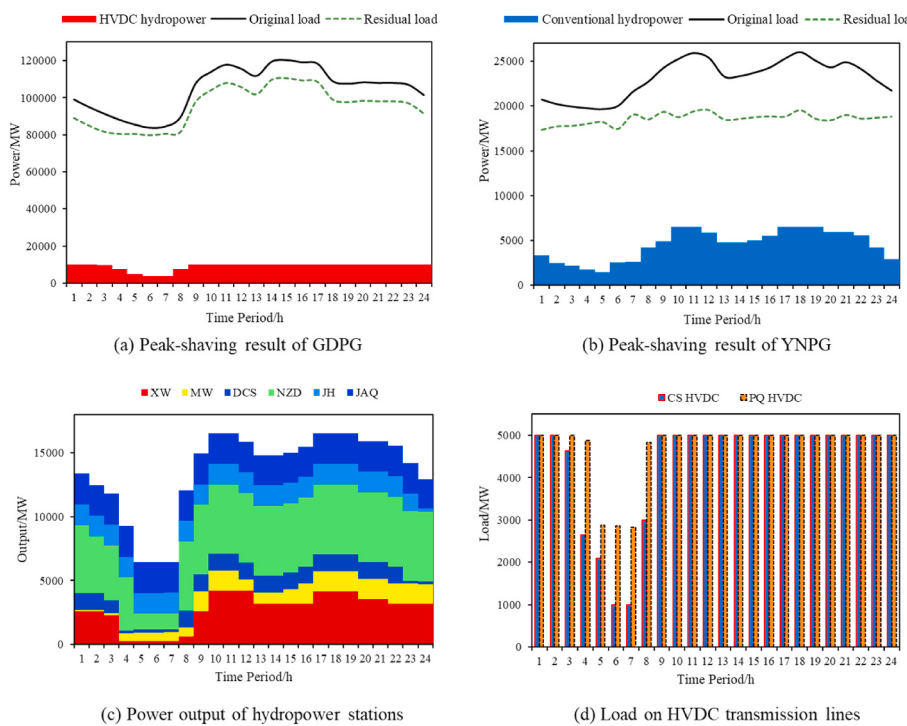


Fig. 4. Optimization result in the flood season.

Table 5
Comparison of HVDC line optimal results in the dry season and flood season.

Items	Dry season		Flood season	
	CS line	PQ line	CS line	PQ line
Electricity transmission/GWh	62.9	62.7	104.3	113.2
Maximum load/MW	5000	5000	5000	5000
Minimum load/MW	500	500	989	2835
Average load/MW	2620	2612	4348	4720
Load rate/%	52%	52%	87%	94%

Table 6
Influence comparison of the results under different R_e .

Items	Power grids	$R_e = 1/1$	$R_e = 1/2$	$R_e = 1/3$	$R_e = 1/4$
Electricity sent/GWh	YNPG	94.3	62.8	47.1	37.8
	GDPG	94.3	125.6	141.3	151.2
Peak-valley difference of residual load/MW	YNPG	2554	3755	6019	5958
	GDPG	23206	21615	20222	20554
Peak-valley difference descent/%	YNPG	66%	50%	20%	21%
	GDPG	20%	25%	30%	29%
Power transmission on HVDC tie lines/MWh	CS line	50.8	59.3	67.9	70.0
	PQ line	43.5	66.3	73.4	81.2

power grids were taken as the study case to verify the model. After analyzing the case study result, the conclusions can be drawn as follows:

- 1) The proposed HCS constraint can be well integrated into the multiple power grids daily peak-shaving model to guarantee the power transmission security of the sending-end power grid, and its concise form can be efficiently solved.
- 2) The MILP model established can make full use of the flexibility of hydropower to efficiently address the multiple power grids peak-shaving problem in different cases within an acceptable computation time.
- 3) After analysis, different electricity receiving ratios strongly affect the operation of hydropower stations and the peak-shaving results of

power grids, and the HCS constraint can effectively avoid the unreasonable operation of the hydropower stations and HVDC tie lines.

With the continuous inclusion of new energies such as solar and wind energy, the uncertainty of them will pose greater challenges to the stability of power grids, which will lead more demand of high-quality flexible power sources like hydropower. We believe that the research in this paper was of substantive significance both at present and in the future.

The limitations of this study include: 1) the optimization was based on hydropower stations, where the unit commitment was not considered; 2) Other types of power sources like wind and solar power were not considered. 3) In reality, the load curves on HVDC tie lines are sometimes given in advance, the model proposed cannot be applied in this case. In the future, more precise operation on the units or introducing other power sources for complementary scheduling can be considered, and how to deal with the condition of pre-determined load curves on HVDC transmission lines is a potential research direction.

Data availability statement

The data used to support this study are available from the corresponding author upon reasonable request.

CRediT authorship contribution statement

Shengli Liao: Methodology, Writing – original draft, Funding acquisition. **Hualong Yang:** Conceptualization, Software, Writing – original draft, Writing. **Benxi Liu:** Data curation, Writing – review & editing, Writing - review, Formal analysis. **Hongye Zhao:** Supervision, Writing – review & editing. **Huan Liu:** Validation. **Xiangyu Ma:** Visualization. **Huijun Wu:** Investigation.

Declaration of competing interest

The authors declare that they have no known competing financial interests or personal relationships that could have appeared to influence

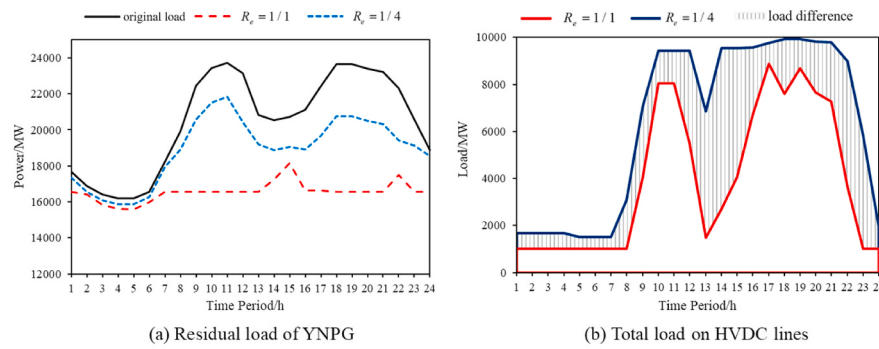
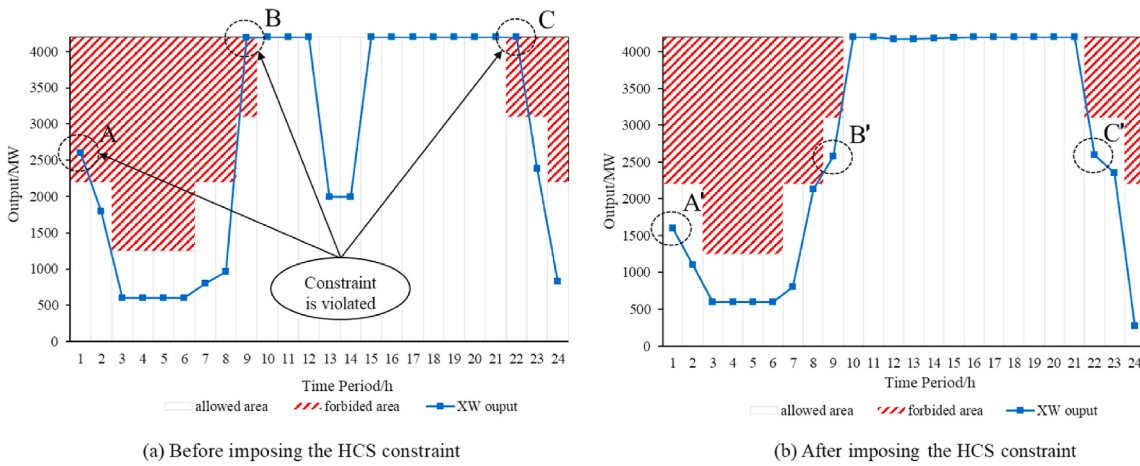
Fig. 5. Operation result under different R_e values.

Fig. 6. Influence of the HCS constraint.

the work reported in this paper.

Acknowledgment

This project was supported by National Natural Science Foundation of China (No. 51979023, No. U1765103) and the Fundamental Research Funds for the Central Universities (No. DUT20JC16).

References

- [1] C. Cheng, J. Shen, X. Wu, K. Chau, Operation challenges for fast-growing China's hydropower systems and response to energy saving and emission reduction, *Renew. Sustain. Energy Rev.* 16 (2012) 2386–2393, <https://doi.org/10.1016/j.rser.2012.01.056>.
- [2] J. Shen, C. Cheng, Q. Shen, J. Lu, J. Zhang, Overview of China's hydropower absorption: evolution, problems, and suggested solutions, *IET Renew. Power Gener.* 13 (2019) 2491–2501, <https://doi.org/10.1049/iet-rpg.2019.0469>.
- [3] A. Alassi, S. Baháne, O. Ellabban, G. Adam, C. MacIver, HVDC transmission: technology review, market trends and future outlook, *Renew. Sustain. Energy Rev.* 112 (2019) 530–554, <https://doi.org/10.1016/j.rser.2019.04.062>.
- [4] A. Kalair, N. Abas, N. Khan, Comparative study of HVAC and HVDC transmission systems, *Renew. Sustain. Energy Rev.* 59 (2016) 1653–1675, <https://doi.org/10.1016/j.rser.2015.12.288>.
- [5] S. Liao, Z. Liu, B. Liu, C. Cheng, X. Wu, Z. Zhao, Daily peak shaving operation of cascade hydropower stations with sensitive hydraulic connections considering water delay time, *Renew. Energy* 169 (2021) 970–981, <https://doi.org/10.1016/j.renene.2021.01.072>.
- [6] S. Liao, Y. Zhang, J. Liu, B. Liu, Z. Liu, Short-term peak-shaving operation of single-reservoir and multicasade hydropower plants serving multiple power grids, *Water Resour. Manag.* 35 (2021) 689–705, <https://doi.org/10.1007/s11269-020-02751-w>.
- [7] Y. Gu, J. Xu, D. Chen, Z. Wang, Q. Li, Overall review of peak shaving for coal-fired power units in China, *Renew. Sustain. Energy Rev.* 54 (2016) 723–731, <https://doi.org/10.1016/j.rser.2015.10.052>.
- [8] P. Wang, W. Yuan, C. Su, Y. Wu, L. Lu, D. Yan, Z. Wu, Short-term optimal scheduling of cascade hydropower plants shaving peak load for multiple power grids, *Renew. Energy* 184 (2022) 68–79, <https://doi.org/10.1016/j.renene.2021.10.079>.
- [9] J. Shen, C. Cheng, X. Cheng, J.R. Lund, Coordinated operations of large-scale UHVDC hydropower and conventional hydro energies about regional power grid, *Energy* 95 (2016) 433–446, <https://doi.org/10.1016/j.energy.2015.12.011>.
- [10] R. Cao, J. Shen, C. Cheng, J. Wang, Optimization model for the long-term operation of an interprovincial hydropower plant incorporating peak shaving demands, *Energies* 13 (2020), <https://doi.org/10.3390/en13184804>.
- [11] M. Xu, L. Wu, H. Liu, X. Wang, Multi-objective optimal scheduling strategy for wind power, PV and pumped storage plant in VSC-HVDC grid, *J. Eng.* 2019 (2019) 3017–3021, <https://doi.org/10.1049/joe.2018.8435>.
- [12] W. Yuan, W. Xin, C. Su, C. Cheng, D. Yan, Z. Wu, Cross-regional integrated transmission of wind power and pumped-storage hydropower considering the peak shaving demands of multiple power grids, *Renew. Energy* 190 (2022) 1112–1126, <https://doi.org/10.1016/j.renene.2021.10.046>.
- [13] J. Shen, C. Cheng, J. Zhang, J. Lu, Peak operation of cascaded hydropower plants serving multiple provinces, *Energies* 8 (2015) 11295–11314, <https://doi.org/10.3390/en81011295>.
- [14] C. Su, C. Cheng, P. Wang, J. Shen, Optimization model for the short-term operation of hydropower plants transmitting power to multiple power grids via HVDC transmission lines, *IEEE Access* 7 (2019) 139236–139248, <https://doi.org/10.1109/ACCESS.2019.2943573>.
- [15] B. Liu, J.R. Lund, S. Liao, X. Jin, L. Liu, C. Cheng, Peak shaving model for coordinated hydro-wind-solar system serving local and multiple receiving power grids via HVDC transmission lines, *IEEE Access* 8 (2020) 60689–60703, <https://doi.org/10.1109/ACCESS.2020.2979050>.
- [16] F. Xu, R. Cao, M. Tu, Y. Zhang, L. Yang, D. Zhang, Scheduling model for inter-regional HVDC tie-line generation and transmission system considering conditional sections, in: 2020 IEEE/IAS Ind. Commer. Power Syst. Asia, I CPS Asia 2020, 2020, pp. 1285–1291, <https://doi.org/10.1109/ICPSAsia48933.2020.9208510>.
- [17] G.P. Adam, T.K. Virana, R. Li, P. Li, G. Burt, S. Finney, Review of technologies for DC grids – power conversion, flow control and protection, *IET Power Electron.* 12 (2019) 1851–1867, <https://doi.org/10.1049/iet-pel.2018.5719>.
- [18] X. Yu, T. Yang, K. Cao, D. Cai, L. Wan, K. Zhou, Y. Wang, R. Ze, Analysis of influence factors on the transmission capability of the yu-e back-to-back VSC-HVDC South channel, 2019 IEEE PES innov. Smart grid technol. Asia, ISGT (2019) 291–295, <https://doi.org/10.1109/ISGT-Asia.2019.8881195>, 2019.
- [19] C. Cheng, S. Liao, Z. Tang, M. Zhao, Comparison of particle swarm optimization and dynamic programming for large scale hydro unit load dispatch, *Energy*

- Convers. Manag. 50 (2009) 3007–3014, <https://doi.org/10.1016/j.enconman.2009.07.020>.
- [20] Z. Feng, W. Niu, C. Cheng, X. Wu, Optimization of hydropower system operation by uniform dynamic programming for dimensionality reduction, Energy 134 (2017) 718–730, <https://doi.org/10.1016/j.energy.2017.06.062>.
- [21] L.E. Schäffer, A. Helseth, M. Korpås, A stochastic dynamic programming model for hydropower scheduling with state-dependent maximum discharge constraints, Renew. Energy 194 (2022) 571–581, <https://doi.org/10.1016/j.renene.2022.05.106>.
- [22] J.P.S. Catalao, S.J.P.S. Mariano, V.M.F. Mendes, L.A.F.M. Ferreira, Scheduling of head-sensitive cascaded hydro systems: a nonlinear approach, IEEE Trans. Power Syst. 24 (2009) 337–346, <https://doi.org/10.1109/TPWRS.2008.2005708>.
- [23] G. Hermida, E.D. Castronovo, On the hydropower short-term scheduling of large basins, considering nonlinear programming, stochastic inflows and heavy ecological restrictions, Int. J. Electr. Power Energy Syst. 97 (2018) 408–417, <https://doi.org/10.1016/j.ijepes.2017.10.033>.
- [24] W. Niu, Z. Feng, C. Cheng, Min-max linear programming model for multireservoir system operation with power deficit aspect, J. Water Resour. Plann. Manag. 144 (2018), 06018006, [https://doi.org/10.1061/\(asce\)wr.1943-5452.0000977](https://doi.org/10.1061/(asce)wr.1943-5452.0000977).
- [25] L. Shang, Y. Shang, L. Hu, J. Li, Performance of genetic algorithms with different selection operators for solving short-term optimized reservoir scheduling problem, Soft Comput. 24 (2020) 6771–6785, <https://doi.org/10.1007/s00500-019-04313-8>.
- [26] L. Liu, Q. Sun, Y. Wang, Y. Liu, R. Wennersten, Research on short-term optimization for integrated hydro-PV power system based on genetic algorithm, Energy Proc. 152 (2018) 1097–1102, <https://doi.org/10.1016/j.egypro.2018.09.132>.
- [27] A. Li, L. Wang, J. Li, C. Ji, Application of immune algorithm-based particle swarm optimization for optimized load distribution among cascade hydropower stations, Comput. Math. Appl. 57 (2009) 1785–1791, <https://doi.org/10.1016/j.camwa.2008.10.016>.
- [28] L. Lakshminarasimman, S. Subramanian, A modified hybrid differential evolution for short-term scheduling of hydrothermal power systems with cascaded reservoirs, Energy Convers. Manag. 49 (2008) 2513–2521, <https://doi.org/10.1016/j.enconman.2008.05.021>.
- [29] B. Tong, Q. Zhai, X. Guan, An MILP based formulation for short-term hydro generation scheduling with analysis of the linearization effects on solution feasibility, IEEE Trans. Power Syst. 28 (2013) 3588–3599, <https://doi.org/10.1109/TPWRS.2013.2274286>.
- [30] C. Cheng, J. Wang, X. Wu, Hydro unit commitment with a head-sensitive reservoir and multiple vibration zones using MILP, IEEE Trans. Power Syst. 31 (2016) 4842–4852, <https://doi.org/10.1109/TPWRS.2016.2522469>.
- [31] Z. Feng, W. Niu, W. Wang, J. Zhou, C. Cheng, A mixed integer linear programming model for unit commitment of thermal plants with peak shaving operation aspect in regional power grid lack of flexible hydropower energy, Energy 175 (2019) 618–629, <https://doi.org/10.1016/j.energy.2019.03.117>.
- [32] H.I. Skjelbred, J. Kong, O.B. Fosso, Dynamic incorporation of nonlinearity into MILP formulation for short-term hydro scheduling, Int. J. Electr. Power Energy Syst. 116 (2020), 105530, <https://doi.org/10.1016/j.ijepes.2019.105530>.